

Generation of magnetic skyrmions through pinning effect

Ji-Chong Yang,¹ Qing-Qing Mao,¹ and Yu Shi^{1,2}

¹*Department of Physics & State Key Laboratory of Surface Physics,
Fudan University, Shanghai 200433, China*

²*Collaborative Innovation Center of Advanced Microstructures, Fudan University,
Shanghai 200433, China*

(Dated: December 15, 2024)

Abstract

On the basis of analytical argument and lattice simulation, we propose that magnetic skyrmions can be generated through the pinning effect in 2D chiral magnetic materials. In our simulation, we find that magnetic skyrmions are generated in the pinning areas and remain stable for a long time. We have studied the properties of the skyrmions with various values of ferromagnetic exchange strength J and the Dzyaloshinskii-Moriya interaction strength D . By using the pinning effect, magnetic skyrmions can be generated in the absence of external magnetic field or magnetic anisotropy at desired positions. This method is useful for the potential applications in magnetic information storage.

PACS numbers: 75.70.Kw, 66.30.Lw, 75.10.Hk, 75.40.Mg

I. INTRODUCTION

The topologically protected structure called skyrmion can be formed in a chiral magnet [1, 2], as discovered in the bulk MnSi by using neutron scattering [3], and also observed by using Lorentz transmission electron microscopy [4] and by using spin-resolved scanning tunnelling microscopy (STM) [5]. They exist in magnetic materials that lack inversion symmetry and are due to Dzyaloshinskii-Moriya (DM) interactions [6]. Magnetic skyrmions can be driven by spin current, and the critical current density to manipulate magnetic skyrmions is lower than for magnetic domain-walls [7], thus they are promising as future information carriers in magnetic information storage and processing devices. Therefore it is very interesting to find out the efficient means of creation and manipulation of magnetic skyrmions.

Single skyrmions can be created and deleted on a $Ir(111)$ surface with the help of local spin-polarized STM [8]. A large number of magnetic skyrmions were created in a short time by constructing a geometrical constriction [9, 10]. An important feature in these works is the presence of magnetic field. On the other hand, skyrmions can also be generated without magnetic field, but using a circulating current [11], and can be generated and stabilized with the help of magnetic anisotropy [12, 13]. They can also be created at desired position with the help of direct current (DC) and with modified magnetic anisotropy even in the absence of DM interaction [14].

Defects and impurities can lead to inhomogeneities of the ferromagnetic exchange coupling J , the DM interaction D , and the magnetic anisotropy [15, 16]. This is the effect of pinning. The modified magnetic anisotropy [14] is an example of the pinning effect on the creation of skyrmions. The creation of skyrmions by using STM [8] can also be regarded as the effect of inhomogeneity of B . Previously, the external magnetic field, the magnetic anisotropy, or a current is needed to generate skyrmions.

In this paper, however, we propose a novel method to generate magnetic skyrmions, only using the inhomogeneity of J . The radii and other properties of the skyrmions are controlled by the parameters of the model, for example, the exchange coupling J and the DM interaction D .

The rest of the paper is organized as the following. In Sec. II we briefly review the 2D magnetic skyrmions and introduce our basic idea. In Sec. III, we report a lattice simulation and study the properties of the skyrmions generated in the simulation. A summary is made

in Sec. IV .

II. BASIC IDEA

It is known that the skyrmions can be generated with the help of magnetic anisotropy, so we only consider the case without magnetic anisotropy. In this case, in the presence of an external magnetic field, the Hamiltonian can be written as as [1, 17]

$$\mathcal{H}_{\text{tot}}(\mathbf{r}) = \frac{\mathbf{J}(\mathbf{r})}{2} (\nabla \mathbf{n})^2 + \mathbf{D}(\mathbf{r}) \mathbf{n} \cdot (\nabla \times \mathbf{n}) - \mathbf{B}(\mathbf{r}) \cdot \mathbf{n}, \quad (1)$$

where \mathbf{n} is the orientation of the local magnetic moment, $J(\mathbf{r})$ is the local ferromagnetic exchange strength, $D(\mathbf{r})$ is the local strength of DM interaction, $\mathbf{B} = B\mathbf{e}_z$ is the external magnetic field along \mathbf{e}_z direction. The local magnetic moment of a skyrmion can be parameterized as [1].

$$\mathbf{n}(x, y) = (\cos(\gamma + m\phi) \sin(\theta(\rho)), \sin(\gamma + m\phi) \sin(\theta(\rho)), g \cos(\theta(\rho))), \quad (2)$$

where ρ and ϕ are polar coordinates of the 2D position vector (x, y) , with the origin of the polar coordinate system at the center of the skyrmion, $m = \pm 1$, $g = \pm 1$, γ is an arbitrary angle, $\theta(\rho)$ is a function describing the shape of a skyrmion, with $\theta(0) = \pi$ and $\theta(\infty) = 0$. The skyrmion charge is defined as [1, 11]

$$Q = \frac{1}{4\pi} \int dx dy \mathbf{n} \cdot \left(\frac{\partial \mathbf{n}}{\partial x} \times \frac{\partial \mathbf{n}}{\partial y} \right) = -mg. \quad (3)$$

It was found previously that for a skyrmion, $\theta(\rho)$ can be approximately described as [18]

$$\theta(\rho) \approx 4 \tan^{-1}(\exp(-a\rho)). \quad (4)$$

Using this expression with $a = 0.05$, some examples of $\mathbf{n}(\mathbf{r})$ are shown in Fig. 1.

Two kinds of pinning were considered previously. In Ref. [15], both J and D are inhomogeneous, while D/J is kept constant. In Ref. [16], D is constant while J is inhomogeneous. For simplicity, we only consider the latter case. Moreover, we only consider the case of $m = 1$. From Eq. (1), for $m = 1$, we find the Euler-Lagrange equation

$$\frac{\sin(\theta) \cos(\theta)}{\rho} - \theta' - \rho \theta'' - 2 \frac{\hat{D}}{J(\rho)} \sin^2(\theta) + \frac{\hat{B}}{J(\rho)} \rho \sin(\theta) - \rho \frac{J'(\rho)}{J(\rho)} \theta' = 0, \quad (5)$$

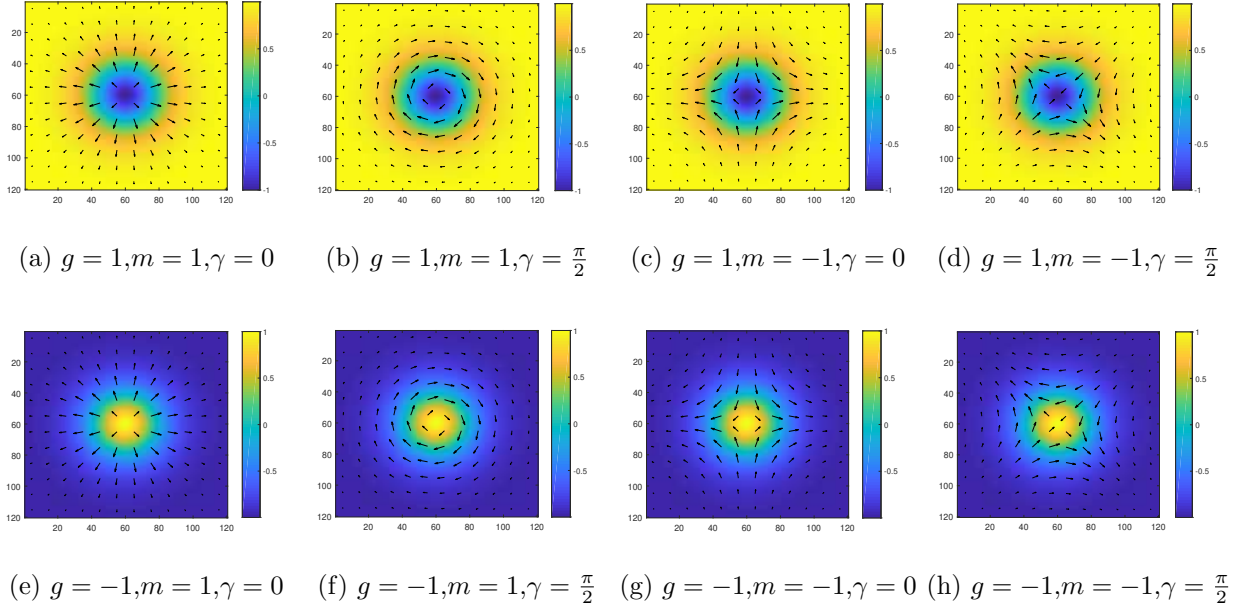


FIG. 1: A skyrmion characterized by $\mathbf{n}(\mathbf{r})$ parameterized as in Eqs. (2) and (4), with various values of g , m and γ . The heat map represents the magnitude of n_z and the arrows represent (n_x, n_y) .

where $\hat{D} \equiv g \sin(\gamma)D$, $\hat{B} \equiv gB$, $J(\rho)$ is a pinning function dependent only on ρ , and it is assumed that the skyrmion center is at the center of the pinning and the pinning is rotationally symmetric. When there is no pinning while an external magnetic field is applied, Eq. (5) becomes

$$\frac{\sin(\theta) \cos(\theta)}{\rho} - \theta' - \rho\theta'' - 2\frac{\hat{D}}{J} \sin^2(\theta) + \frac{\hat{B}}{J} \rho \sin(\theta) = 0. \quad (6)$$

It is known that, in this case the skyrmions can be generated.

We note that when pinning is present, J' term in Eq. (5) may play a role as the \hat{B} term. For example, suppose $\hat{B} = 0$ but the pinning has the form of

$$J(\rho) = J_0 + b \frac{a\rho + \log(e^{-2a\rho} + 1)}{a^2}, \quad (7)$$

where a is the same as a in Eq. (4), J_0 and b are undetermined coefficients. Then with ansatz (4), Eq. (5) becomes

$$\frac{\sin(\theta) \cos(\theta)}{\rho} - \theta' - \rho\theta'' - 2\frac{\hat{D}}{J(\rho)} \sin^2(\theta) + \frac{b}{J(\rho)} \rho \sin(\theta) \approx 0. \quad (8)$$

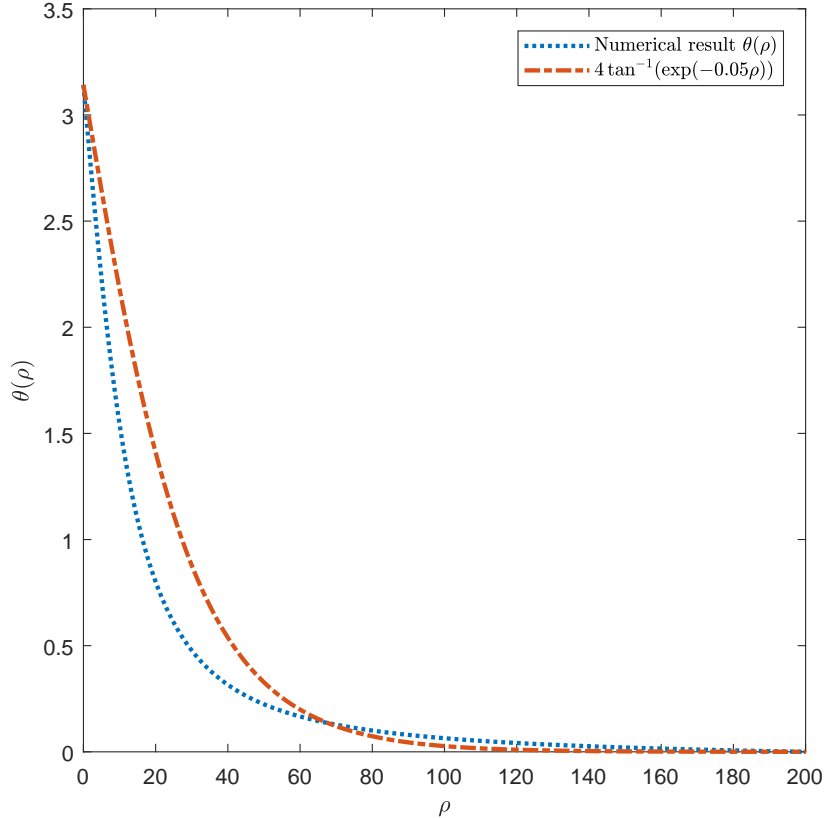


FIG. 2: The dotted line represents the numerical result of Eq. (5) with $\hat{B} = 0$. The dashed line represents the skyrmion ansatz (4).

which is very close to the Eq. (6) except that the J is position dependent in (5) while j is position independent in (6). Using the numerical method introduced in Ref. [15], we solved Eq. (5) with $J(\rho)$ given in Eq. (7) and with parameter values $J_0 = 1$, $\hat{B} = 0$, $\hat{D} = 0.05$, $b = 0.005$, $a = 0.05$. As shown in Fig. 2, the solution is very close to skyrmion ansatz (4), suggesting that it is possible to create a skyrmion by using pinning effect.

III. LATTICE SIMULATION

The above investigation, with an artificial pinning effect, suggests the possibility of creating a skyrmion using pinning effect only. We now consider a more realistic pinning effect. As a local structure, the effect of pinning should be suppressed very quickly in deviating from the pinning center. An exponentially decaying function $J(\rho)$ is assumed in Ref. [16],

while a Gaussian function $J(\rho)$ is assumed in Ref. [15]. We follow Ref. [15] to assume $J(\rho)$ has Gaussian form,

$$J(\rho) = J_0 + J_1 e^{-J_2 \rho^2}, \quad (9)$$

where J_0 , J_1 and J_2 are undetermined coefficients with $J_0 > 0$, $J_1 > -J_0$ and $J_2 > 0$. The radius of the pinning is denoted as R_p , and $R_p \sim 1/\sqrt{J_2}$. In this paper, we use dimensionless parameters, and always set $J_0 = 1$ for simplicity.

The effective parameter \hat{D} depends on not only the DM interaction D but also the parameters of the skyrmions, and whether a solution of $\theta(\rho)$ can be identified as a skyrmion is technically subtle. Therefore rather than solving the Euler-Lagrange equation, we perform a lattice simulation, which directly provides evidence of skyrmions. The lattice simulation is based on the Landau-Lifshitz-Gilbert (LLG) equation [1, 15, 19]

$$\frac{d}{dt} \mathbf{n}_{\mathbf{r}} = -\mathbf{B}_{\text{eff}}(\mathbf{r}) \times \mathbf{n}_{\mathbf{r}} - \alpha \mathbf{n}_{\mathbf{r}} \times \frac{d}{dt} \mathbf{n}_{\mathbf{r}}, \quad (10)$$

where $\mathbf{n}_{\mathbf{r}}$ is the local magnetic momentum at grid \mathbf{r} , α is the Gilbert damping constant, \mathbf{B}_{eff} is the effective magnetic field

$$\mathbf{B}_{\text{eff}}(\mathbf{r}) = -\frac{\delta H}{\delta \mathbf{n}_{\mathbf{r}}}, \quad (11)$$

where the discrete Hamiltonian H can be written as [20]

$$H = \sum_{\mathbf{r}, i=x,y} [-J(\mathbf{r}) \mathbf{n}_{\mathbf{r}+\delta_i} - D(\mathbf{r}) \mathbf{n}_{\mathbf{r}+\delta_i} \times \mathbf{e}_i - \mathbf{B}] \cdot \mathbf{n}_{\mathbf{r}}, \quad (12)$$

where δ_i refers to each neighbour, and $\delta_i = \mathbf{e}_i$ on a square lattice. So [15]

$$\begin{aligned} \mathbf{B}_{\text{eff}}(\mathbf{r}) = & \sum_{i=x,y} [J(\mathbf{r}) \mathbf{n}_{\mathbf{r}+\delta_i} + J(\mathbf{r} - \delta_i) \mathbf{n}_{\mathbf{r}-\delta_i}] \\ & + \sum_{i=x,y} [D(\mathbf{r}) \mathbf{n}_{\mathbf{r}+\delta_i} \times \mathbf{e}_i - D(\mathbf{r} - \delta_i) \mathbf{n}_{\mathbf{r}-\delta_i} \times \mathbf{e}_i] + \mathbf{B}(\mathbf{r}). \end{aligned} \quad (13)$$

We run the simulation on a 512×512 square lattice with open boundary condition, and with $\mathbf{B} = 0$. The center of the pinning is set to be at the point (256, 256). In the following, we denote the time step as $d\tau$, and the steps the simulation take is denoted as τ . The simulation is running on the GPU. Compared with the programs running on the CPU, the GPU has a great advantage on this problem.

A. The case of $J_1 > 0$.

We first run the simulation for $J_1 = 3$, $J_2 = 0.001$ and various values of D , starting with randomized \mathbf{n}_r and stopping when \mathbf{n}_r become stable. Previously, the Gilbert constant is taken as $\alpha = 0.01$ to 1 [15, 18, 21–24]. We find that the larger the value of α , the more rapid the simulation can be done, and that the smaller the value of D , the longer it takes for \mathbf{n}_r to become stable. Hence we use $\alpha = 0.1$ [22] and $d\tau = 0.002$ for $D \geq 0.1$, while use $\alpha = 0.2$ [15, 23] and $d\tau = 0.01$ for $D < 0.1$.

1. Skyrmions can be generated.

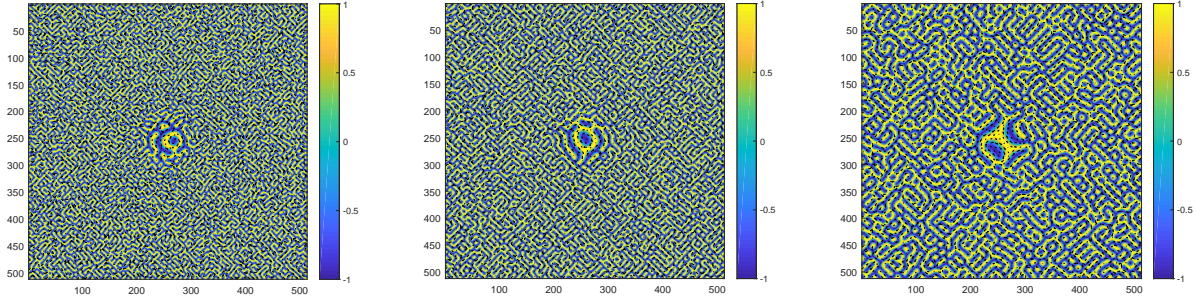
The results are shown in Fig. 3. We run the simulation for $D = 1, 0.8, 0.5, 0.2, 0.1, 0.08, 0.05, 0.03, 0.02, 0.01$. Among each of these runs, a skyrmion is generated at the center of the pinning except when $D = 0.02$ or 0.01 . When D is smaller, it takes longer time to generate the skyrmion. Generally, it takes longer time to generate a skyrmion compared with the generation of skyrmions by using the external magnetic field.

In our simulation, it is easy to generate a skyrmion, but it does not always appear in each run of the simulation, because the initial state is randomized. Fig. 4 shows two examples that the simulation failed to generate a skyrmion at the pinning center, as the skyrmion-like structure in the center cannot be ‘cut off’ from the helicity phase. Although the skyrmion is not generated, the structure of \mathbf{n}_r in the central region is significantly different from elsewhere.

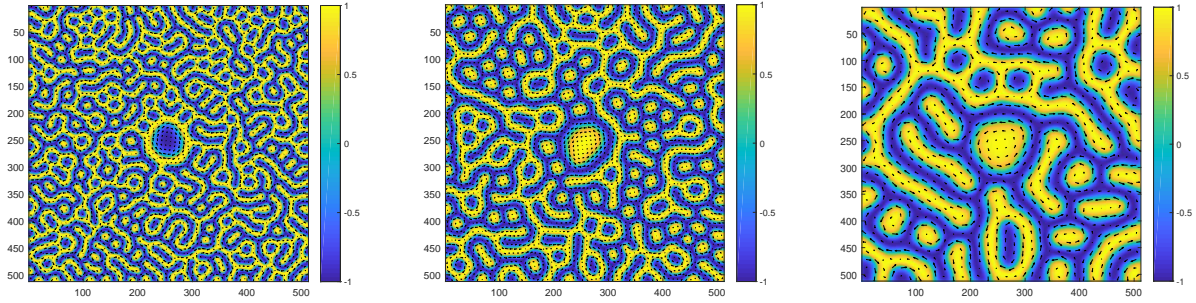
We also study the properties of the skyrmions generated in the simulation. We only study the skyrmions nearest to of the pinning centers. The value of g is determined by n_z at the center of the skyrmions. The radius R_s of each skyrmion is estimated from the radius of the iso-height contour with $n_z = \mp 0.9$ for $g = \pm 1$. The angle γ and m is determined by using n_x and n_y at the iso-height contour with $n_z = 0$.

2. Radii of the skyrmions.

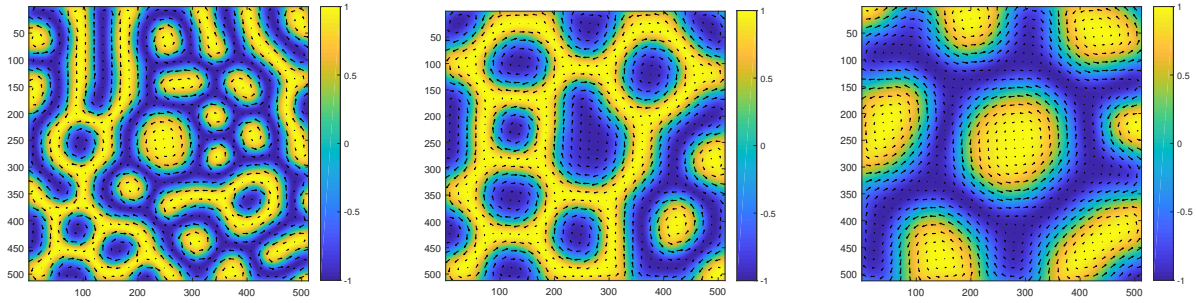
We first investigate the relation between the skyrmion radius R_s and the DM interaction strength D . We find that the larger the value of D , the smaller R_s . The relation between



(a) $D = 1, \tau = 60000, g = 1, m = 1, \gamma \approx 1.58, R_s \approx 10.5$ (b) $D = 0.8, \tau = 500000, g = 1, m = 1, \gamma \approx 1.56, R_s \approx 15.4$ (c) $D = 0.5, \tau = 5000000, g = 1, m = 1, \gamma \approx 1.57, R_s \approx 20.3$

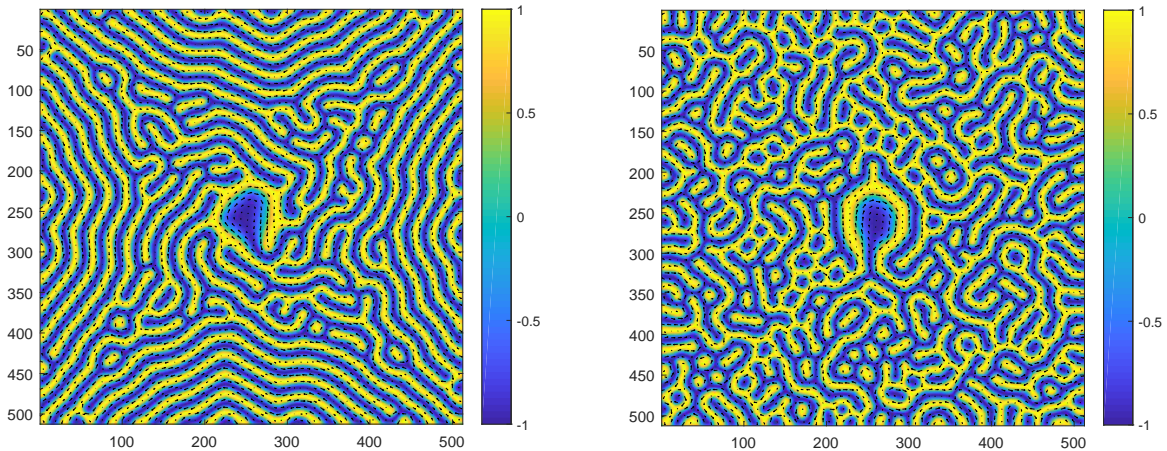


(d) $D = 0.3, \tau = 1500000, g = 1, m = 1, \gamma \approx 1.57, R_s \approx 34.4$ (e) $D = 0.2, \tau = 5000000, g = -1, m = 1, \gamma \approx 4.72, R_s \approx 42.6$ (f) $D = 0.1, \tau = 8000000, g = -1, m = 1, \gamma \approx 4.71, R_s \approx 59.8$



(g) $D = 0.08, \tau = 3000000, g = -1, m = 1, \gamma \approx 4.71, R_s \approx 64.8$ (h) $D = 0.05, \tau = 10000000, g = 1, m = 1, \gamma \approx 1.57, R_s \approx 96.7$ (i) $D = 0.03, \tau = 10000000, g = -1, m = 1, \gamma \approx 4.71, R_s \approx 128.3$

FIG. 3: The simulation result of \mathbf{n}_r , for $J_1 = 3$ and various values of other parameters. We find that the skyrmions can be generated at the pinning centers, by pinning effect only.



(a) Start from $\mathbf{n}_r = \mathbf{e}_z, \tau = 1500000$

(b) Start from randomized $\mathbf{n}_r, \tau = 3000000$

FIG. 4: Two examples that the skyrmion-like structure in the central region cannot be ‘cut off’ from the helicity phase. Although the skyrmion is not generated, the structure of \mathbf{n}_r in the central region is significantly different from elsewhere.

R_s and D can be fitted by $a + b/\sqrt{D}$, as shown in Fig. 5.

Then we study the relation between R_s and the radius $R_p \sim \sqrt{1/J_2}$ of the pinning, as well as that between R_s the distance d between the pinning center and the skyrmion center. As shown in Fig. 6, we run the simulation for $D = 0.3$ and different values of J_2 , and find that the skyrmion radius is more relevant with d than J_2 , and R_s is smaller when d is larger. For the same value of d , R_s decreases with the decrease of pinning radius R_p .

3. Skyrmion numbers and \hat{D} .

We find $m = 1$ for all the skyrmions appearing in the simulation, then with $Q = -mg$, the skyrmion number only depends on the sign of g . As shown in Fig. 3, both $g = \pm 1$ skyrmions can be generated. For a skyrmion generated by an external magnetic field, g depends on the direction of \mathbf{B} . But for a skyrmion generated by using the pinning effect in absence of a magnetic field, the sign of g becomes a free choice and depends on the initial state (Figs. 7, 8).

For $D > 0$, we find that for $g = 1$, $\gamma \approx \pi/2$, while for $g = -1$, $\gamma \approx -\pi/2$. Hence $\hat{D} > 0$ in both cases. We also run simulations with $D < 0$ (Fig. 9), in which $\hat{D} > 0$ is also valid for

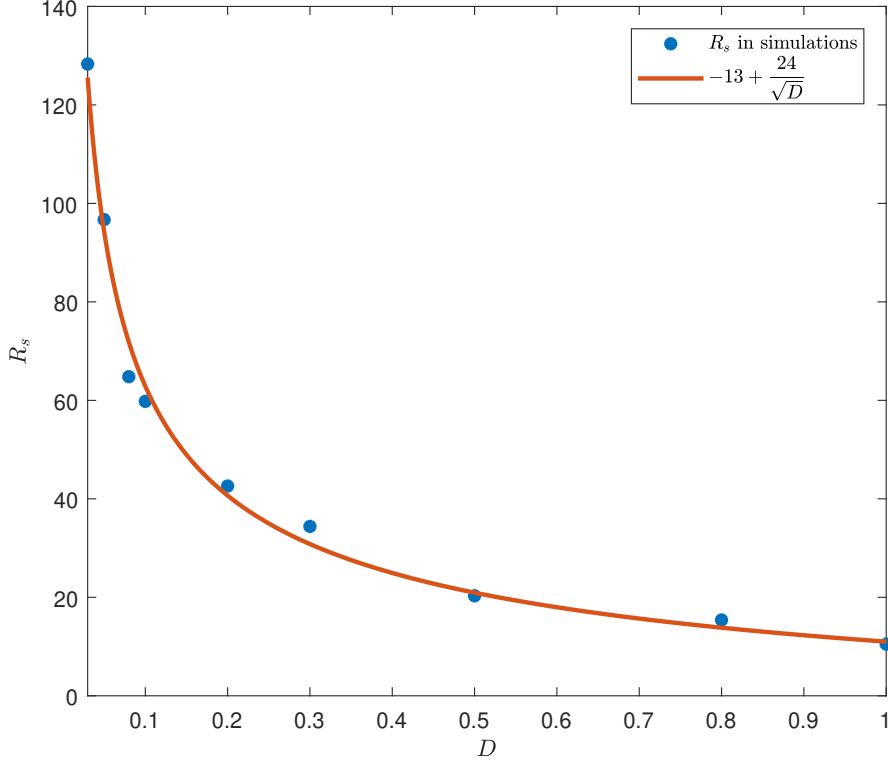


FIG. 5: The fitted relation between skyrmion radius R_s and the DM interaction strength D .

the skyrmions generated. This can be understood from

$$H_{\text{DM}} = D\mathbf{n} \cdot (\nabla \times \mathbf{n}) = gD \sin(((m-1)\phi + \gamma) \left(\frac{m}{2\rho} \sin(2\theta(\rho)) + \theta'(\rho) \right)), \quad (14)$$

which differs from the $g = 1$ case [1] by replacing D as gD . As a result, the sign of g is a free choice, while the sign of γ is determined by gD . Hence the energy is lowest when $\hat{D} > 0$, $m = 1$ and $\gamma = \pm\pi/2$, with the sign of γ determined by gD . $\gamma = \pi/2$ when $gD > 0$, $\gamma = -\pi/2$ when $gD < 0$.

4. The process of the skyrmion generation.

The process of the skyrmion generation is interesting. We show two examples with $D = 0.1$ and $D = 0.03$ in Figs. 10 and 11, respectively. When D is too small, the width of the strip in the helicity state is large compared with the radius of the pinning, and the pinning effect is small. On the other hand, when D is large, it is known that the external magnetic field to generate skyrmions is approximately $B \sim D^2/J$ [25] when D is large. Since

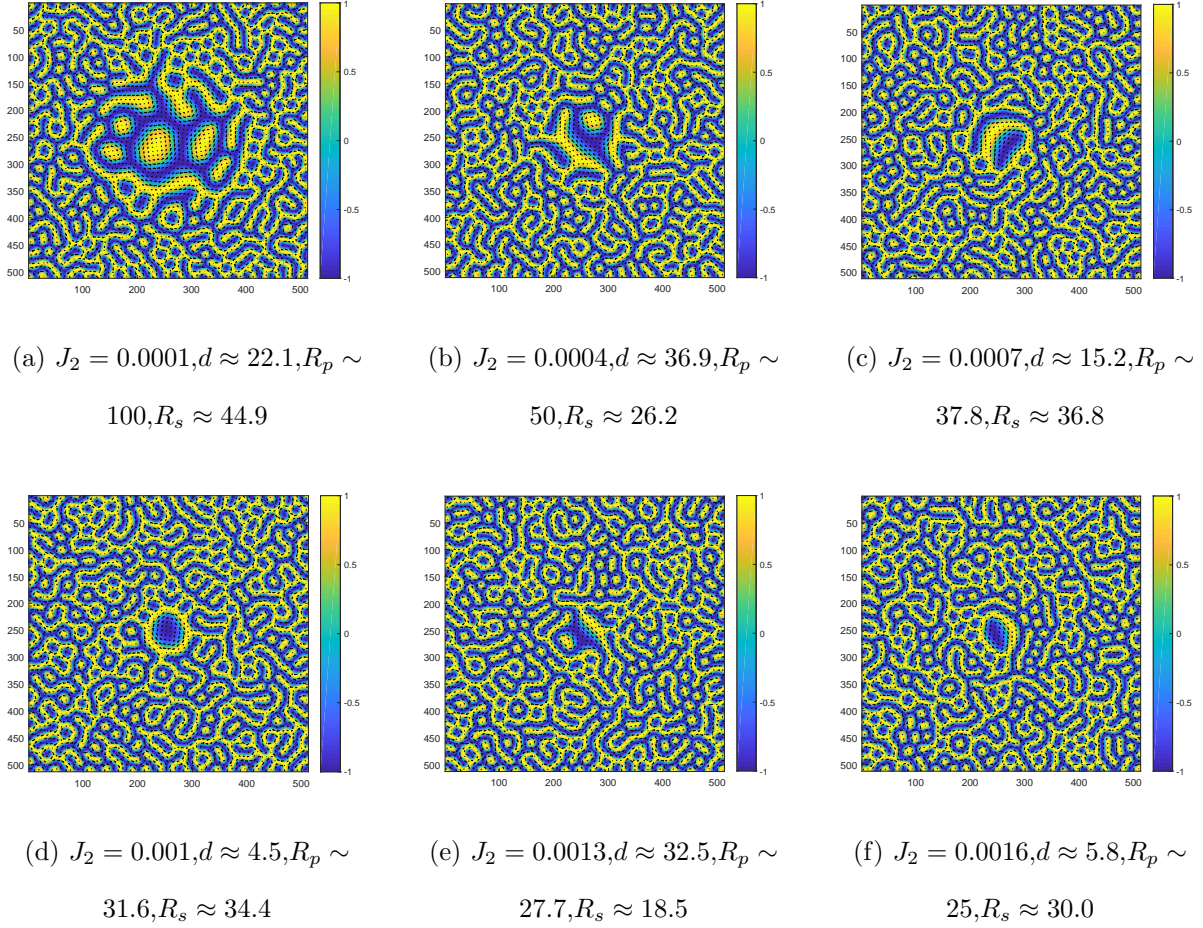


FIG. 6: The simulation for $D = 0.03$ and various values of J_2 . $\tau = 1500000$. $R_p \sim \sqrt{1/J_2}$ is the radius of the pinning center. d is the distance between the centers of the skyrmion and the pinning. R_s is more relevant with d other than with R_p . When d is about the same, R_s is a monotonic function of R_p . The result shown in (d) is also the result shown in Fig. 3. (d).

the pinning plays role as B , a large value of J' is needed to generate skyrmions when D is large. As a result, we conclude that, with $J(\rho)$ fixed, the skyrmions can only be generated when the value of D is appropriate.

When the value of D is appropriate, and when the strip of the helicity state is formed over the region of the pinning, different parts of the strip receive different effects from the pinning, i.e., the strip is thicker at the center of the pinning and is thinner at the edge of the pinning. As a result, an olive-shaped structure can be formed near the center of the pinning. It is known that the skyrmions can be dragged to the center of the pinning [15].

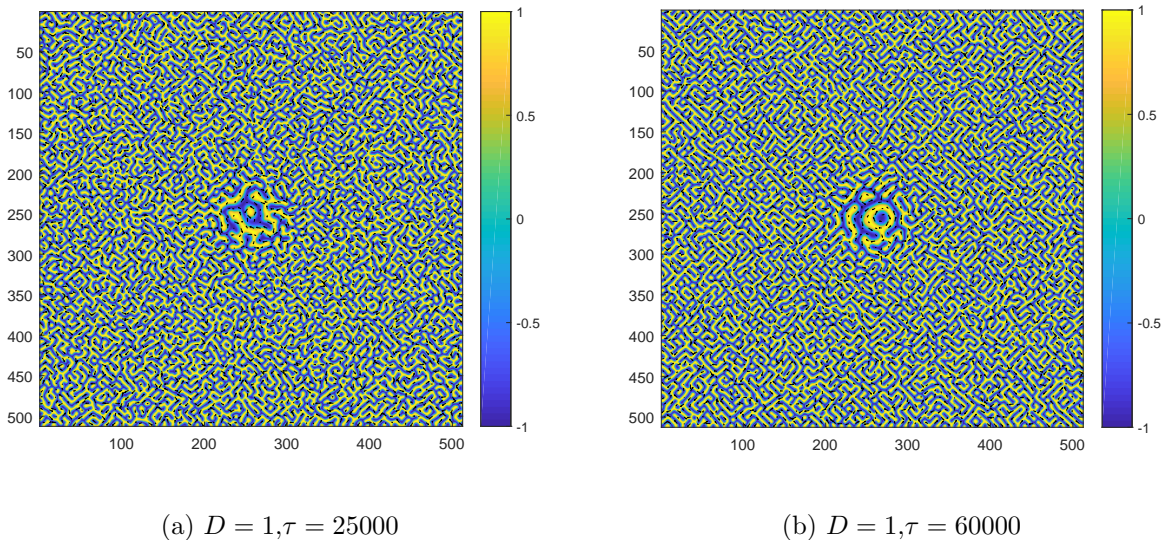


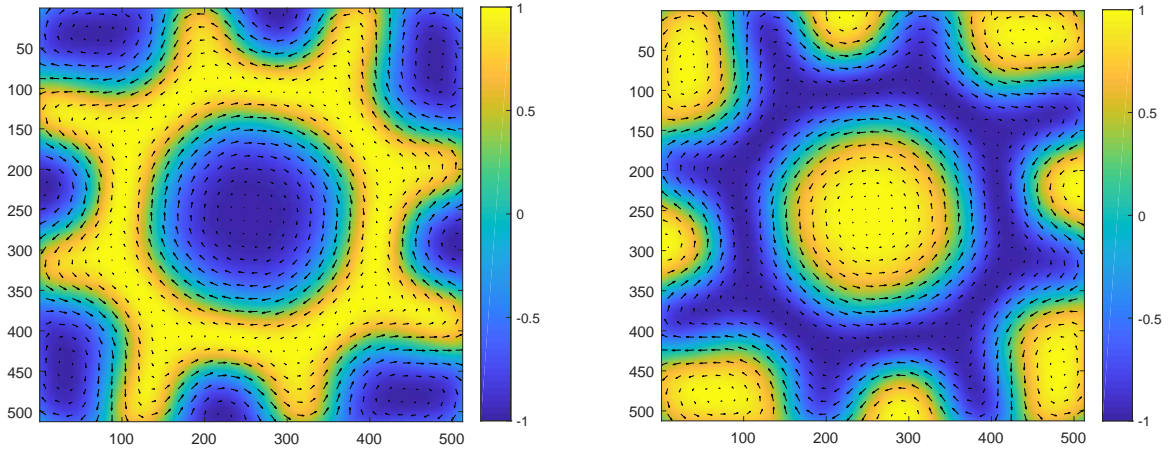
FIG. 7: Two simulations with randomized initial states and the same values of all the other parameters. Both $g = 1$ and $g = -1$ skyrmions can be generated, depending on the initial state. The result in Fig. 7. (b) is the same result in Fig. 3. (a).

When it is dragged to the center, the olive-shaped structure can possibly be cut off from the stripand becomes a skyrmion. As shown in Figs. 10 and 11, at the beginning of simulation, several olive-shaped structures are generated, and one of them is dragged into the center of the pinning and its shape becomes more symmetric because of the rotational symmetry of $J(\rho)$.

B. The case of $J_1 < 0$.

1. The properties of the skyrmions when $J_1 < 0$.

We also study the case of $J_1 < 0$. Using $J_1 = -0.5$, $J_2 = 0.0001$, $\alpha = 0.2$, $d\tau = 0.01$, we find the skyrmions generated in the simulation (Fig. 12). In this case, the possible range of D in which skyrmions can be generated is narrower than the case of $J_1 = 3$ and $J_2 = 0.001$. As in the case of $J_1 > 0$, the radius of the skyrmion increases with the decrease of D . However, the skyrmions generated in large distance from the pinning center is larger than in the case of $J_1 > 0$. Same as the case when $J_1 > 0$, we also find $m = 1$ and $\hat{D} > 0$ for all the skyrmions generated in case $J_1 < 0$.



(a) Start from \mathbf{n} all point up.

(b) Start from \mathbf{n} all point down.

FIG. 8: Simulations for $D = 0.03$, starting from $\mathbf{n}_r = \mathbf{e}_z$ and from $\mathbf{n}_r = -\mathbf{e}_z$. The result provides further evidence that the sign of g depends on the initial state.

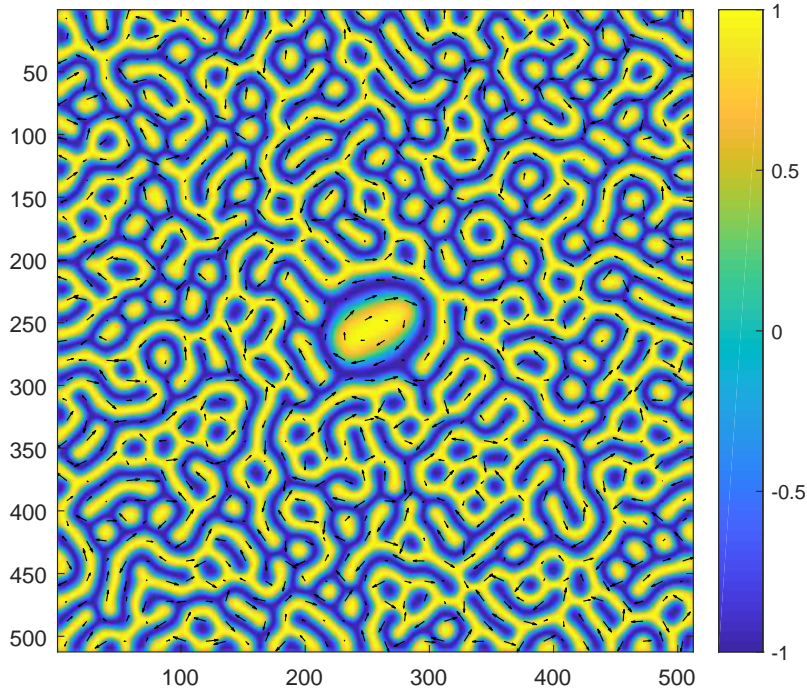


FIG. 9: The simulation for $D = -0.3$, $\tau = 2000000$. The skyrmion generated at the center has the properties $m = 1$, $g = -1$, $\gamma \approx 1.55$, and thus $\hat{D} \approx 0.3$.

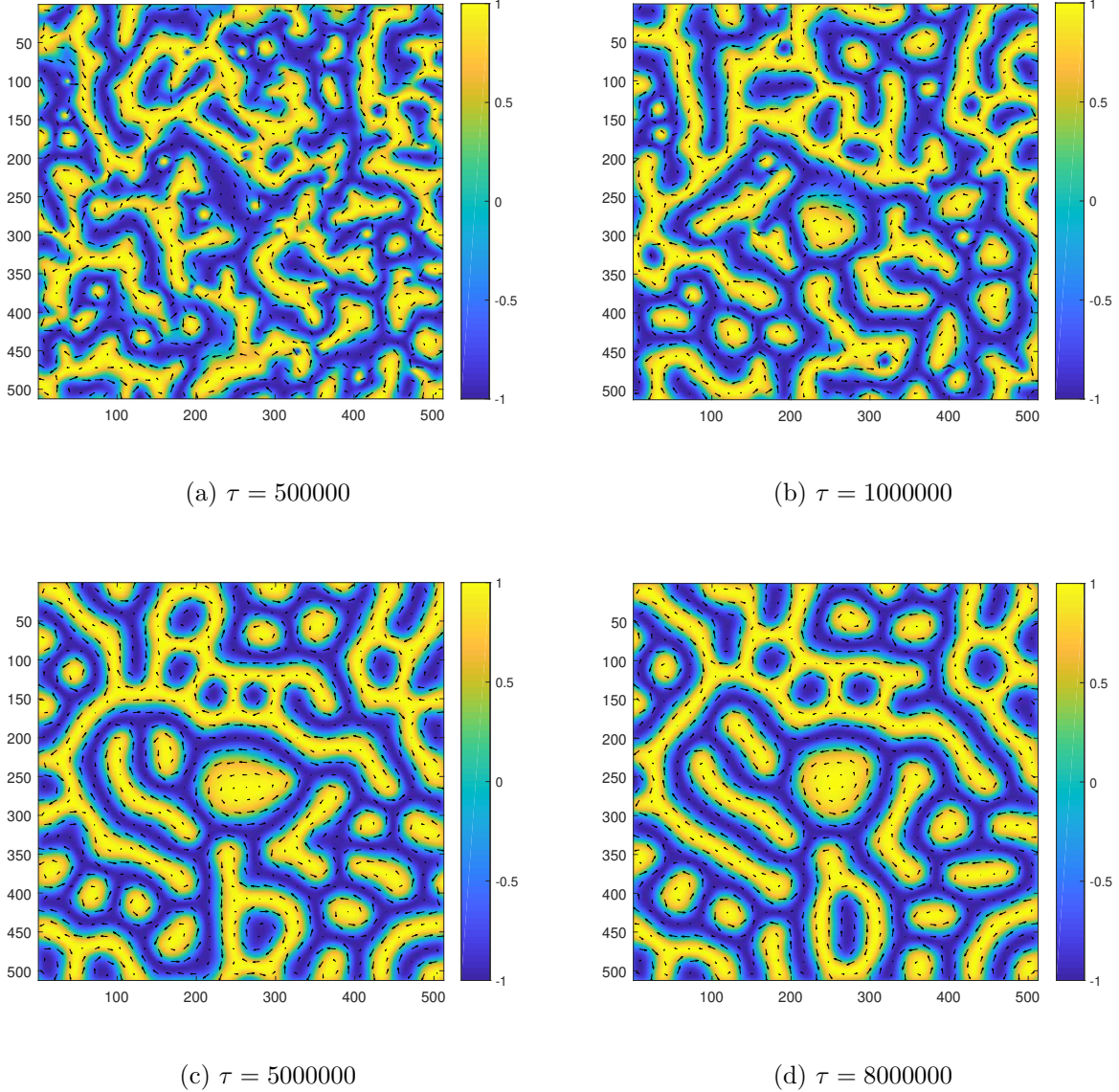


FIG. 10: The process of skyrmion generation for $D = 0.1$. (d) is as same as Fig. 3. (f).

2. The bound state phenomenon.

We also observe an interesting phenomenon when D is very small in the case of $J_1 < 0$ (Figs. 13 and 14), which does not show up in the case of $J_1 > 0$. When D is very small, two skyrmions with $g = 1$ and $g = -1$ are generated and move to the pinning center. They keep rotating around each other with the distance shrinking till annihilation. Previously, it was found that the interaction between two skyrmions on two layers with opposite skyrmion charge can form a bound state [24]. The situation we consider may provide another stage

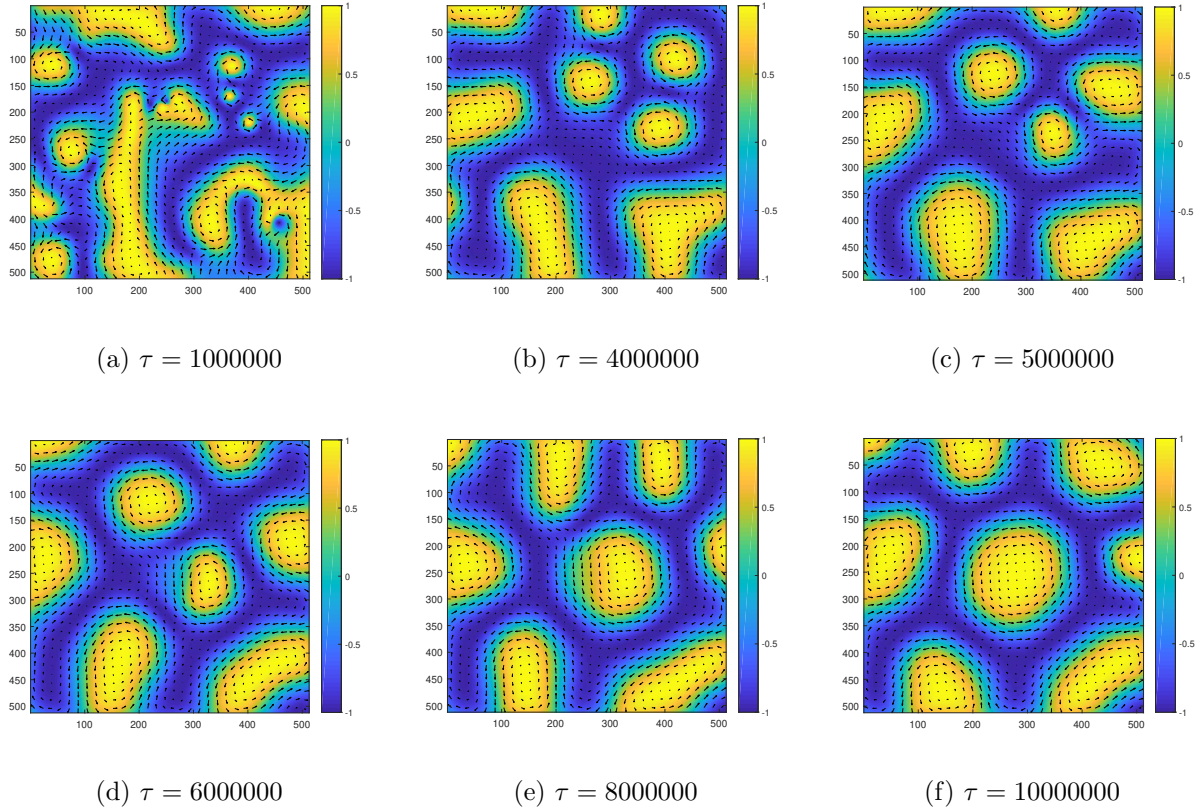


FIG. 11: The process of skyrmion generation for $D = 0.03$. (f) is as same as Fig. 3. (i).

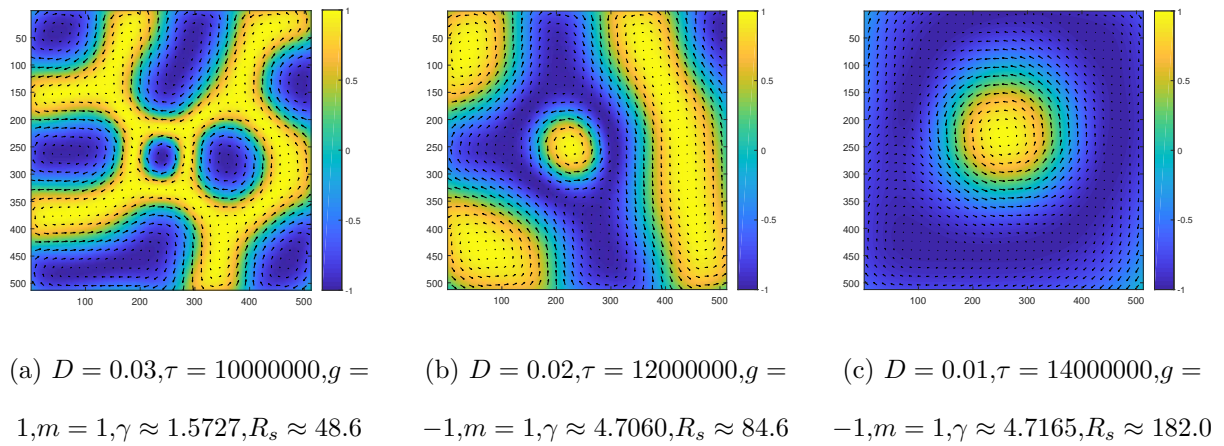


FIG. 12: Simulation result of \mathbf{n}_τ for $D = 0.3, 0.2, 0.1, 0.03$. The heat map represents the magnitude of n_z , the arrow represents (n_x, n_y) . In (a), we estimate the radius and γ of the skyrmion at the center.

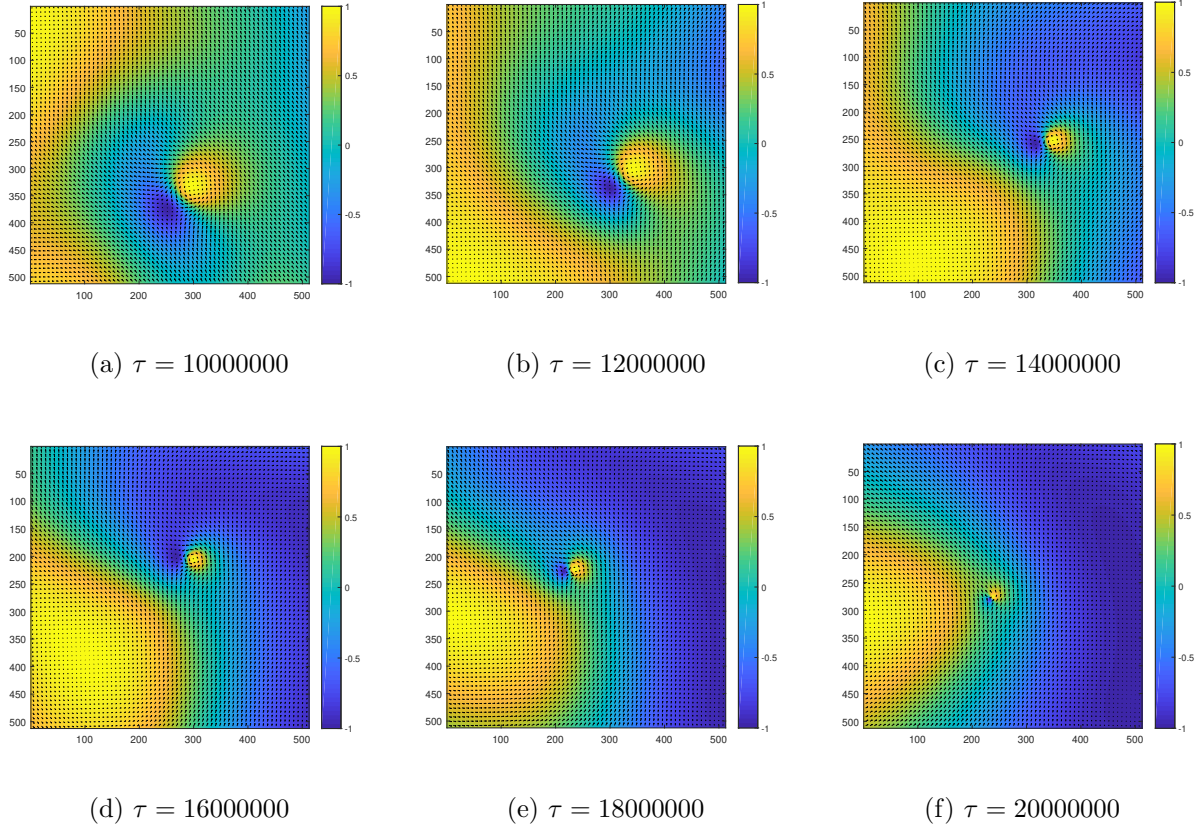


FIG. 13: Simulation of skyrmion generation, with parameter values $J_1 = -0.5$, $J_2 = 0.0001$, $D = 0.005$, $\alpha = 0.2$ and $d\tau = 0.01$. Two skyrmions with $g = 1$ and $g = 1$ respectively rotate around each other and move to the pinning center, with the distance shrinking till annihilation.

to study skyrmion bound states.

IV. SUMMARY

In this paper, we propose a novel mechanism to generate magnetic skyrmions without needing the external magnetic field or magnetic anisotropy. We find that skyrmions can be generated through the pinning effect only, i.e., with the inhomogeneous magnetic exchange strength J . Our lattice simulation has verified this idea. In the simulation, we study the properties of the skyrmions generated under various parameter values. We find that the radius of the skyrmion increases when D decrease. For $J_1 > 0$, the closer the skyrmions to the pinning center, the larger the sizes of the skyrmions. For $J_1 < 0$, the sizes are smaller.

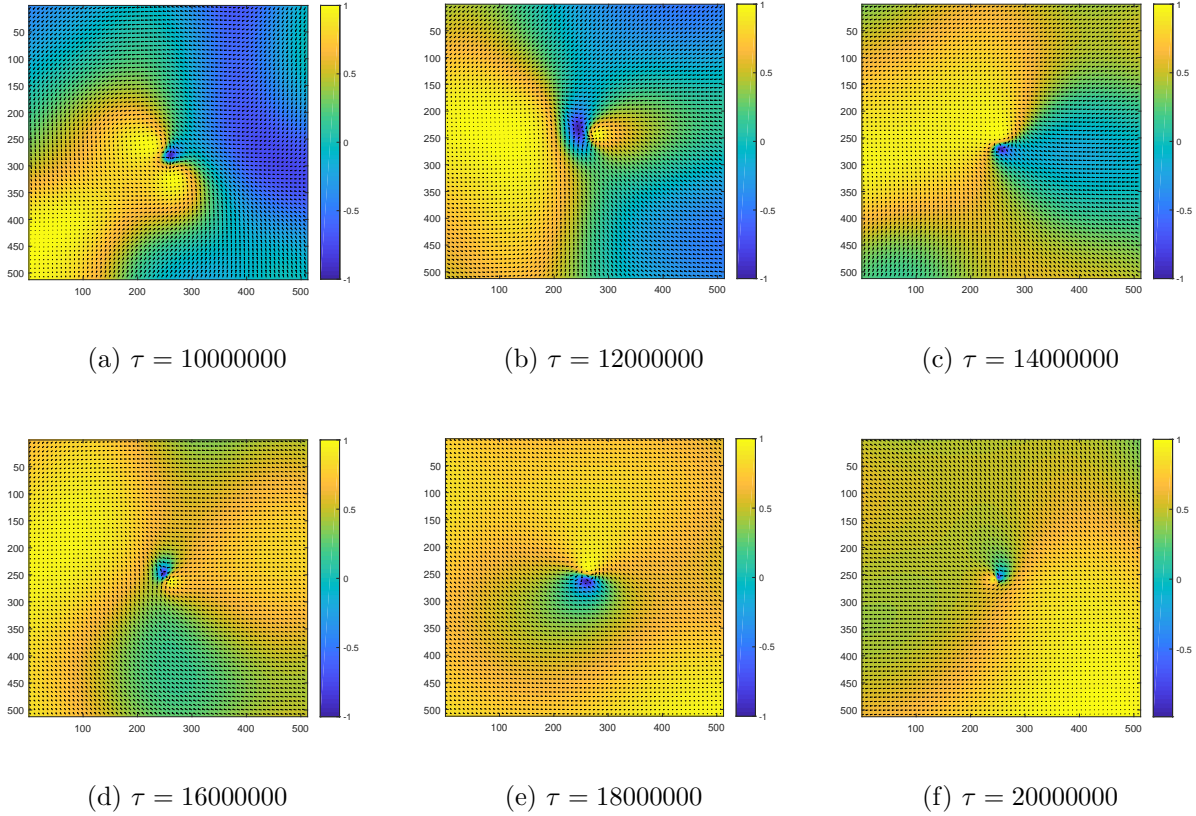


FIG. 14: Simulation of skyrmion generation, with parameter values $J_1 = -0.9$, $J_2 = 0.0001$, $D = 0.003$, $\alpha = 0.1$ and $d\tau = 0.01$. Two skyrmions with $g = 1$ and $g = 1$ respectively are generated at the pinning center. Each skyrmion self rotates. This simulation stopped at $\tau = 20000000$, however, as the distance shrinks, it expected the pair will annihilate.

We also find that all skyrmions generated have $m = 1$ and $\hat{D} > 0$, while the sign of g depend on the initial state. For $J_1 < 0$, we also find the generation of a pair of skyrmions with opposite charges at the pinning center.

The phenomenon that the skyrmions can be generated by using the pinning effect only is useful for practical applications of the magnetic skyrmions. Through the engineering of pinning in the designated site, we can generate a skyrmion on this site. It is hoped that experiments and applications be made by using this method.

This work is supported by National Natural Science Foundation of China (Grant No. 11374060 and No. 11574054).

-
- [1] N. Nagaosa and Y. Tokura, *Nat. Nanotechnol.* **8**, 899 - 911 (2013).
- [2] A. Fert, N. Reyren and V. Cros, *Nat. Rev. Mater.* **2**, 17031 (2017).
- [3] S. Mühlbauer et. al. *Science* **323**, 915 - 919 (2009).
- [4] X. Z. Yu et. al. *Nature* **465**, 901 - 904 (2010).
- [5] S. Heinze et. al. *Nature Phys.* **7**, 713 - 718 (2011);
C. Pfleiderer, *Nature Phys.* **7**, 673 - 674 (2011).
- [6] I. Dzyaloshinskii, *J. Phys. Chem. Solids* **4**, 241 - 255 (1958);
T. Moriya, *Phys. Rev.* **120**, 91 - 98 (1960).
- [7] F. Jonietz et. al. *Science* **330**, 1648 - 1651 (2010);
X. Z. Yu et. al. *Nature Commun.* **3**, 988 (2012).
- [8] N. Romming et. al. *Science* **341**, 636 - 639 (2013).
- [9] W. Jiang et. al. *Science* **349**, 283 - 286 (2015).
- [10] W. Jiang et. al. *Physics Reports*, **704**, 1 - 49 (2017), arXiv:1706.08295.
- [11] Y. Tchoe and J. H. Han, *Phys. Rev. B.* **85**, 174416 (2012), arXiv:1203.0638.
- [12] A. Bogdanov and A. Hubert, *J. Magn. Magn. Mater.* **195** 182 (1999).
- [13] X. Zhang et. al. *Nat. Commun.* **7**, 10293 (2016), arXiv:1504.02252.
- [14] K. Everschor-Sitte et. al. *New J. Phys.* **19**, 092001, (2017), arXiv:1610.08313.
- [15] Y.-H. Liu and Y.-Q. Li, *J. Phys. Condens. Matter* **25** 076005 (2013).
- [16] S. Z. Lin et. al. *Phys. Rev. B* **87**, 214419 (2013).
- [17] J. H. Han et. al. *Phys. Rev. B* **82**, 094429 (2010).
- [18] R. Nepal, U. Güngördü and A. A. Kovalev, *Appl. Phys. Lett.* **112**, 112404 (2018),
arXiv:1711.03041.
- [19] G. Tatara, H. Kohno and J. Shibata, *Phys. Rep.* **468**, 213 - 301 (2008), arXiv:0807.2894;
J. Zang et. al. *Phys. Rev. Lett.* **107** 136804 (2011).
- [20] J. Iwasaki, M. Mochizuki, and N. Nagaosa, *Nat. Nanotechnol.* **8**, 742 - 747, (2013),
arXiv:1310.1655;
J. Iwasaki, M. Mochizuki, and N. Nagaosa, *Nature Commun.* **4**, 1463, (2013);
M. Mochizuki, *Phys. Rev. Lett.* **108**, 017601 (2012), arXiv:1111.5667.
- [21] J. Sampaio et. al. *Nat. Nanotechnol.* **8**, 839, (2013);

- K. Litzius et. al. Nat. Phys. **13**, 170 - 175 (2016);
- W. Jiang et. al. Nat. Phys. **13**, 162 - 169 (2016), arXiv:1603.07393;
- S. Huang et. al. Phys. Rev. B **96** 144412 (2017);
- [22] R. Tomasello et. al. J. Phys. D: Appl. Phys. **50** 325302 (2017);
- S. H. Yang et. al. Nat. Nanotechnol. **10**, 221, (2015);
- J. Barker and O. A. Tretiakov, Phys. Rev. Lett. **116** 147203 (2016).
- [23] C. Schütte et. al. Phys. Rev. B **90** 174434 (2014).
- [24] W. Koshibae and N. Nagaosa, Sci. Rep. **7** 42645 (2017).
- [25] J. H. Han et. al. Phys. Rev. B **82** 094429 (2010), arXiv:1006.3973.